

CALIBRATION OF MODEL OF FLOW AND HEAT PRODUCTION INSIDE A COMBUSTION ENGINE*

Jiří Maryška, Josef Novák, Jan Šembera

*Department of Modelling of Processes
Technical University of Liberec
Liberec, Czech Republic
jan.sembera@vslib.cz*

ABSTRACT

A short description of the calibrated model of compressible flow, diffusive-advective mass and heat transport, and combustion inside the cylinder of a combustion engine is made and results of its calibration for one measured test are presented.

The first part of the article is devoted to the structure and a brief description of the model. The problem is modelled by a sequence of three isochoric processes (changes of flow and pressure fields by finite element method, transport of mass and heat by finite volume method, and heat production and mass change by ordinary differential equation model) and adiabatic volume change (represented by change of mesh and re-computation of all fields of physical properties due to adiabatic process).

In the second part of the article, there is the calibration of modelled global energy production with measured data described and its result shown. Then the conclusion from the results is done.

NOMENCLATURE

A_1, \dots, A_N ... the species appearing in the model
 $c_i(\mathbf{x}, t)$... field of the mass fraction of the i^{th} specie in the gas mixture
 N ... number of species appearing in the model
 $\mathbf{n}(\mathbf{x}, t)$... outward normal vector to boundary $\Gamma(t)$ in the point $\mathbf{x} \in \Gamma(t)$
 $p(\mathbf{x}, t)$... pressure field
 t ... time
 $T(\mathbf{x}, t)$... temperature field
 $\mathbf{v}(\mathbf{x}, t) = (v_1, v_2, v_3)$... velocity field
 $\mathbf{x} = (x_1, x_2, x_3)$... vector of position in space
 $\Gamma(t) = \partial\Omega(t)$... the boundary of engine cylinder
 $\rho(\mathbf{x}, t)$... mass density field

* This work was supported with the subvention from Ministry of Education of the Czech Republic, project code 242200001.

$\Omega(t)$... time-dependent domain of engine cylinder

INTRODUCTION

The final aim of our modelling is to predict production of nitrogen oxides from an internal combustion engine. For this purpose, a precise chemical reaction model should be developed. Its main inputs would be flow, temperature, and pressure fields and their development in time. This contribution is devoted to a model of relevant physical processes, which is being developed at Technical University of Liberec and whose outputs would form such inputs to the precise chemical reaction model. It is being built as a model of compressible flow, transport of mass and energy, and production of energy in a time-dependent domain.

A short overview of the model is done in the next section. The rest of the paper is focused to one specific problem – the simplified model of combustion. It is modelled applying strong simplification on the reaction rate, as described in the subsection Model of chemical processes. To verify that such simplification can be done, one real problem was measured and the simplified model was calibrated to compute as near data as possible.

OVERVIEW OF THE MODEL

The volume and shape of the cylinder of engine change in time. To simplify the problem, we discretize it in time and in each time step we split the solution into two stages, isochoric and adiabatic one. All modelled processes are computed in the isochoric stage, supposed to take place in a fixed domain:

- production of mass and energy by chemical reactions,
- compressible flow of gas mixture,
- mass and energy transport.

All of them are discretized in time and space and solved by either finite volume or finite element method. The spatial computational mesh, built up of trilateral prismatic elements/volumes in layers, is common to all models (see Figure 1).

The adiabatic stage models an immediate change of volume. Its key procedure is change of computational mesh. A more detailed description of the setting of the model can be found in [1].

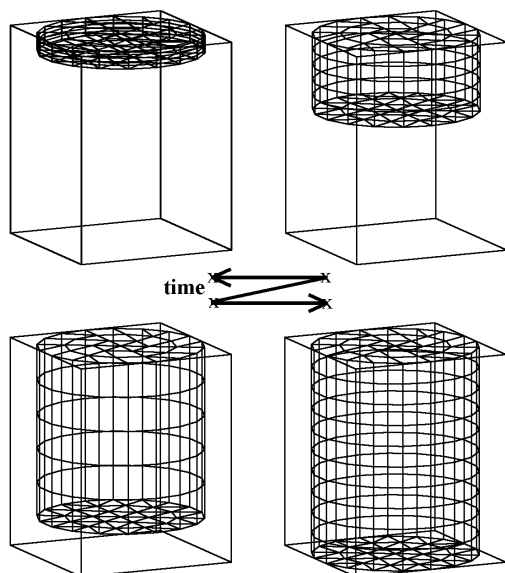
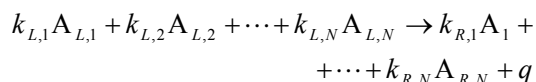


Figure 1. Schematic example of computational mesh in four time steps

Model of chemical processes

All chemical processes are described by the set of stoichiometric equations where each one can be written as



where $k_{L,i}$ and $k_{R,j}$ are stoichiometric coefficients of reagents and products A_i . During this reaction, the heat q is produced. It can be positive or negative depending on the type of such reaction.

Local kinetic equations for a computation of mass and energy production can be expressed by linear ordinary differential equations

$$\frac{dc_i}{dt} = -\bar{R} m_i (k_{L,i} - k_{R,i}), \quad \frac{dT}{dt} = \bar{R} \frac{q}{C_V},$$

where m_i is the molar mass of reagent A_i , C_V is the isochoric heat capacity of the gas mixture (evaluated as a cubic function of temperature) and \bar{R} is the reaction rate generally depending on many parameters as mass fractions of all components of the gas mixture, temperature, pressure, etc.

Simplified model of the reaction rate \bar{R} supposes it as a function of only temperature, mass fractions, and logical function \mathfrak{I} expressing ignition:

$$\bar{R}(T, \{c_j\}_{j=1}^N, \mathfrak{I}) = \begin{cases} 0 & \text{for } ((T < T_C) \& (-\mathfrak{I})) \\ & \text{or } (\exists j = 1, \dots, N) \\ & (k_{L,j} > 0 \& c_j = 0) \\ \bar{\bar{R}}(c_L) & \text{otherwise} \end{cases}$$

Parameter T_C (so-called critical temperature) controls initiation of the reaction – the reaction starts by increasing of the local temperature over T_C .

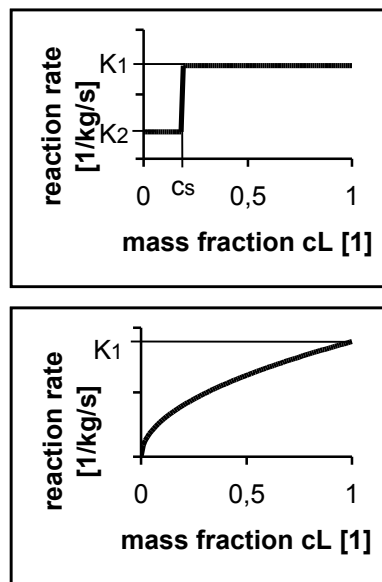


Figure 2. Basic reaction rate models "A" and "B"

Four basic reaction rate $\bar{\bar{R}}$ models, depending only on mass fraction of chosen "burning specie" L, were implemented: here denoted simply "A", "B", "C", and "D" (see

Figure 2 and Figure 3) – they all are parameterised by 1 to 3 parameters (reference rate K_1 [1/kg/s], change mass fraction c_s [1], and second reference rate K_2 [1/kg/s]).

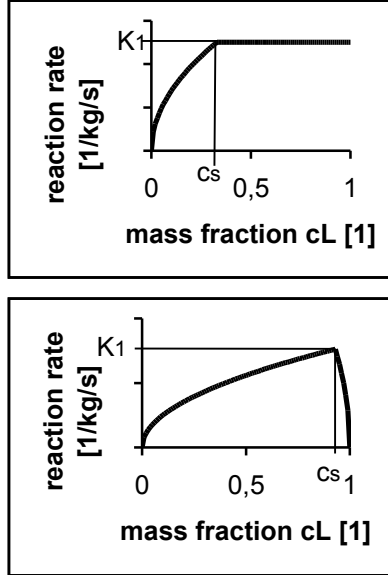


Figure 3. Basic reaction rate models “C” and “D”

Two ignition models of logical function \mathfrak{I} were tested: ellipsoid artificial ignition and spark ignition. The spark ignition is natural one (it is parameterised by the time-of-spark t_{sp} – see Figure 5). The ellipsoid ignition (parameterised by start-time t_{sp} and ignition-time t_{ig}): $\mathfrak{I}_{el}(\mathbf{x}, t) =$

$$\begin{cases} 0 & \text{when } (\mathbf{x} - \mathbf{x}_{sp}) \cdot \mathbf{A}(t)(\mathbf{x} - \mathbf{x}_{sp}) > \frac{t - t_{sp}}{t_{ig}} \\ 1 & \text{when } (\mathbf{x} - \mathbf{x}_{sp}) \cdot \mathbf{A}(t)(\mathbf{x} - \mathbf{x}_{sp}) \leq \frac{t - t_{sp}}{t_{ig}} \end{cases}$$

where \mathbf{x}_{sp} is the central point of upper side of the cylinder, $\mathbf{A}(t) = \frac{1}{2} \text{diag}(r, r, h(t))$, where r is radius of engine cylinder and $h(t)$ is its height in time t – see Figure 4) was implemented to artificially model development of fire inside the cylinder to save computational time. Computations using this artificial ignition are made without computing flow field and mass and energy transport, which consume most of computational time.

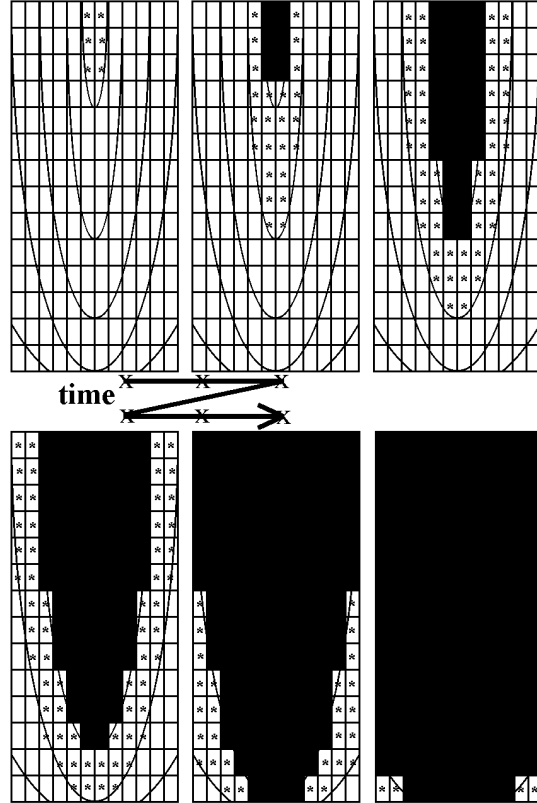


Figure 4. Ellipsoid artificial ignition shown in a vertical cross-section of the cylinder (blank field means that in the domain is $\mathfrak{I} = \text{false}$, star means that \mathfrak{I} is just being switched to **true**, full field is $\mathfrak{I} = \text{true}$)

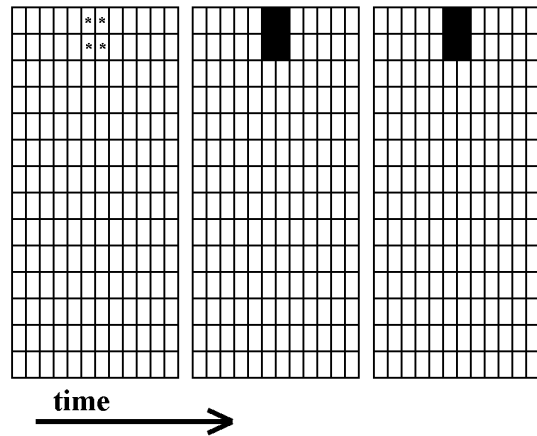


Figure 5. Spark ignition shown in a vertical cross-section of the cylinder (blank field means that in the domain is $\mathfrak{I} = \text{false}$, star means that \mathfrak{I} is just being switched to **true**, full field is $\mathfrak{I} = \text{true}$)

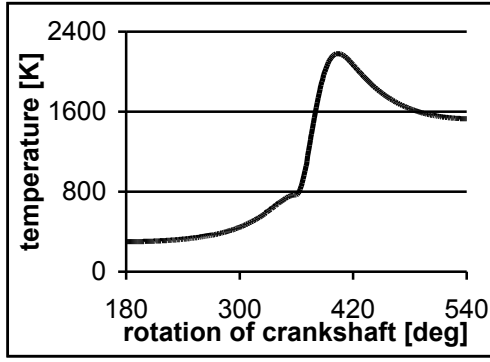


Figure 6. Development of temperature inside the cylinder of the engine processed from measurements.

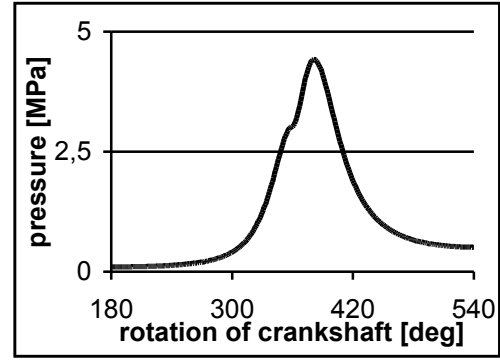


Figure 7. Development of pressure inside the cylinder of the engine processed from measurements.

Fluid flow model

The model of flow of compressible gas mixture is governed by the set of Navier-Stokes equations, the continuity equation, and the state equation of perfect gas [2]:

$$\begin{aligned} \frac{\partial \mathbf{v}}{\partial t} + (\mathbf{v} \cdot \mathbf{grad}) \mathbf{v} &= \nu \Delta \mathbf{v} + \tilde{\nu} \mathbf{grad} \operatorname{div} \mathbf{v} - \frac{1}{\rho} \mathbf{grad} p \\ \frac{\partial \rho}{\partial t} + \operatorname{div}(\rho \mathbf{v}) &= 0, \\ p &= \tilde{R} T \rho. \end{aligned}$$

Here \mathbf{v} is the velocity vector, p pressure of gas, ρ its density, T is temperature, and \tilde{R} , ν , $\tilde{\nu}$ are molar gas constant and two viscosity coefficients of the gas mixture.

The system is solved in fixed 3D-domain $\Omega(t_i)$ in the time-interval (t_i, t_{i+1}) with initial and boundary conditions:

$$\begin{aligned} T(t=t_i) &= T_0, \quad \rho(t=t_i) = \rho_0, \quad \mathbf{v}(t=t_i) = \mathbf{v}_0, \\ \mathbf{v} \cdot \mathbf{n} - \sigma(p - p_D) &= v_N \text{ on } \Gamma_N \subset \partial\Omega(t_i), \\ p &= p_D \text{ on } \Gamma_D \subset \partial\Omega(t_i), \end{aligned}$$

where Γ_N and Γ_D are disjoint and covering parts of the boundary and $\mathbf{n}(\mathbf{x})$ is the outward normal to the boundary.

Non-linear system is discretized by mixed hybrid finite element method and linearized. Formulation of the model is set in [1], global behaviour tests were successfully performed and further testing is being in process.

Model of mass and energy transport

The mass and energy transport is governed by the set of mass balance equations for each component of the gas mixture and the transport energy [3]:

$$\begin{aligned} C_V \left[\frac{\partial}{\partial t} (\rho T) + \operatorname{div}(\rho T \mathbf{v}) \right] - \operatorname{div}(k \mathbf{grad} T) &= \\ &= C_V T^+ \gamma_+ - C_V T \gamma_- - \tilde{R} \rho T \operatorname{div} \mathbf{v} + \\ &+ \mu \sum_{i,j} \left[\frac{\partial v_j}{\partial x_i} + \frac{\partial v_i}{\partial x_j} - \frac{2}{3} \operatorname{div} \mathbf{v} \right] \frac{\partial v_j}{\partial x_i} \\ \frac{\partial}{\partial t} (\rho c_i) &= \operatorname{div}(\rho D_i \mathbf{grad} c_i) - \operatorname{div}(\rho c_i \mathbf{v}) + \\ &+ c_i^+ \gamma_+ - c_i \gamma_- \end{aligned}$$

in a given flow field $\mathbf{v}(\mathbf{x}, t)$ for unknown functions $\rho(\mathbf{x}, t)$, $c_i(\mathbf{x}, t)$ ($i=1, \dots, N$). N is the number of components of gas mixture, γ_+ denotes the density of sources (with defined mass fractions c_i^+ and temperature T^+), γ_- is the (positive) density of sinks, D_i is the diffusion coefficient of the i^{th} specie in the gas mixture, $\mu = \rho \nu$ is absolute viscosity coefficient.

The problem is solved in fixed 3-D domain $\Omega(t_i)$ in the time-interval (t_i, t_{i+1}) with initial and boundary conditions:

$$\rho(t=t_i) = \rho_0, \quad c_j(t=t_i) = c_{0,j}, \quad T(t=t_i) = T_0,$$

$$\left. \begin{aligned} c_j &= c_{j,D}, j = 1, \dots, N \\ \rho &= \rho_D \\ T &= T_D \end{aligned} \right\} \text{on } \Gamma_{in} \subset \partial\Omega(t_i),$$

$$\left. \begin{aligned} \mathbf{grad} c_j \cdot \mathbf{n} &= 0, j = 1, \dots, N \\ \mathbf{grad} T \cdot \mathbf{n} &= 0 \end{aligned} \right\} \text{on } \Gamma_{out} \subset \partial\Omega(t_i)$$

where Γ_{in} and Γ_{out} are the inlet and the rest parts of the boundary and $\mathbf{n}(\mathbf{x})$ is the outward normal to the boundary.

The problem is solved using upwind explicit finite volume method. The scheme is conservative. Its disadvantages are strong restriction for the time step and numerical diffusion. Both are analysed and partially solved in [4].

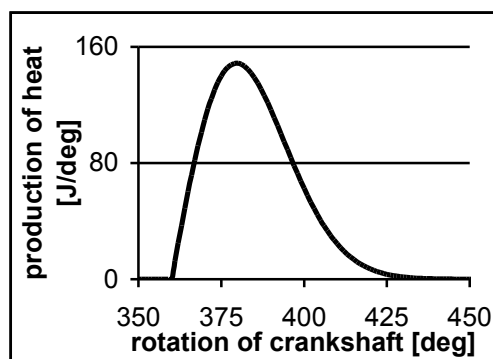


Figure 8. Graph of ideal production of energy inside the gas combustion engine \tilde{q}_a corresponding to measured temperature and pressure.

CALIBRATION OF THE CHEMICAL REACTION MODEL

To verify that it is possible to apply simplified local reaction rate model, one test problem was defined according to data from measurements, we have had. All parameters of the numerical model having their physical meaning were set according to the measured engine (the parameters were e.g. dimensions of the engine, speed of the engine, capacity of the methane fuel, mass fractions of methane, oxygen, and other gases in the initial time, stoichiometry of the reaction of burning of methane etc.), discretization parameters (length of the time step, number of finite elements/volumes,

number of iterations of linearized computation of flow) were set to allow make as many and as credible computations as possible, and remaining parameters should be calibrated (ignition parameters – start-time and ignition-time or time-of-spark – kind of the basic local reaction rate model, its parameters – K_1 , K_2 , c_s – and critical temperature T_C).

The calibration was made in the following steps:

- choice of the basic local reaction rate model;
- choice of ellipsoid artificial ignition parameters;
- choice of basic reaction rate model parameters;
- choice of critical temperature (T_C) parameter.

As the optimised criterion, the sum of quadrates of difference between computed and measured integrated energy produced from the start of engine cycle chosen, i.e.

$$\text{error} = \sum_{\alpha=1}^{720} (Q_\alpha - \tilde{Q}_\alpha)^2 \text{ [J}^2\text{]}, \text{ where}$$

$$Q_\alpha = \sum_{a=1}^{\alpha} q_a \text{ [J]} \quad \text{and} \quad \tilde{Q}_\alpha = \sum_{a=1}^{\alpha} \tilde{q}_a \text{ [J]}.$$

Here q_a [J/deg] and \tilde{q}_a [J/deg] denote computed and measured production of energy in whole cylinder of the engine in the time interval, in which the crankshaft rotates 1 degree from $a-1$ to a degrees.

This criterion was found better than comparison of rate of instantaneous energy

production $\sum_{\alpha=1}^{720} (q_\alpha - \tilde{q}_\alpha)^2$, since the difference

between integrals shows “how far” from the desired time the energy was produced. On the Figures 6 - 8, there can be seen the data processed from measurement, which were to be fitted. Figure 7 represents measured development of pressure in a real methane engine, temperature on Figure 6 and the Wiebe ideal production of energy \tilde{q}_a with parameters fitted to measured data on Figure 8 were obtained from the 0D model of development of pressure and temperature. The 0D model is based on Wiebe model of production of energy. It computes change of global pressure and global temperature common to whole cylinder of engine as a sequence of adiabatic and isochoric changes governed by equations of ideal gas, but C_V is

evaluated as function depending on temperature. It is described (in Czech only) in [5].

Choice of the basic reaction rate model

Making a sparse set of 3389 computations with ellipsoid ignition model and various other parameters, we have found that the best results are reached using the basic reaction rate model "A". In the Table 1, the results are shown ("minimal error" means the minimal error obtained from the whole set of computations with various parameters, the last column contains the ratio between the corresponding minimal error and "A" minimal error, the error expressed in per mille is computed as square root of ratio of error

$$\text{in } J^2 \text{ and the sum } \sum_{\alpha=1}^{720} \tilde{Q}_{\alpha}^2 = 3\,459\,179\,230 \text{ J}^2).$$

Table 1. Results of choosing of basic reaction rate model.

basic reaction rate model	minimal error [J ²] / [%]	min. error/ least min. error
"A"	94 852 / 5,2	1,00
"C"	130 213 / 6,1	1,37
"D"	220 520 / 8,0	2,32
"B"	629 842 / 13,5	6,64

Choice of the ignition parameters

For further computations, the basic reaction rate model "A" and ellipsoid ignition model were used. 1512 various combinations of parameters of both models were tested. First couple of the best computational results is shown in Table 2. The column "error/least error" contains the ratio of corresponding error and the least one in the whole sample. The last column "finish time" shows the sum of start-time and ignition-time. It can be seen that the first best 21 results have the finish-time either 193 or 194 degrees, and that the first computation with different finish-time has almost twice as large error than the least one.

Next, another set of test computations was defined for finish-time 193 or 194 degrees. The first 22 results are written in Table 3. The concluding decision was to use the following parameters of the ignition model:
start-time = 173 degrees,
ignition-time = 21 degrees.

Table 2. Results of calibration of start-time and ignition-time – the finish-time observation (all time data are expressed in degrees of rotation of crankshaft, K₁ and K₂ are expressed in 1/kg/s)

start time [deg]	ignition time [deg]	K ₁	cs [1]	K ₂	error [J ²]	error/ least error	finish time [deg]
173	21	86	0.18	290	73959	1.00	194
172	22	91	0.18	285	85349	1.15	194
172	22	86	0.18	280	87422	1.18	194
172	22	86	0.18	285	88042	1.19	194
174	20	86	0.18	290	89612	1.21	194
174	19	91	0.18	285	94852	1.28	193
175	18	91	0.18	285	94852	1.28	193
172	22	91	0.18	280	96274	1.30	194
173	21	91	0.18	290	96926	1.31	194
172	22	96	0.18	285	98016	1.33	194
174	19	96	0.18	285	101298	1.37	193
175	18	96	0.18	285	101298	1.37	193
174	19	86	0.18	285	104358	1.41	193
175	18	86	0.18	285	104358	1.41	193
174	20	91	0.18	290	110629	1.50	194
172	22	96	0.18	280	115949	1.57	194
173	21	96	0.18	285	120118	1.62	194
173	21	91	0.18	285	124463	1.68	194
173	21	96	0.18	290	129399	1.75	194
173	20	86	0.18	280	129400	1.75	193
174	20	96	0.18	290	141432	1.91	194
175	17	86	0.18	280	142317	1.92	192

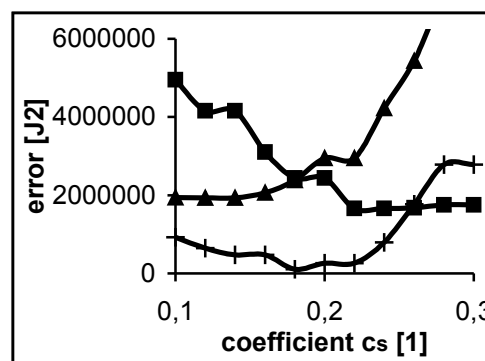


Figure 9. Selected curves of dependence of error on the coefficient c_s. Curve with "+" marks is the one containing optimal solution.

Choice of the reaction rate model parameters

The next 1030 computations were performed for the basic reaction rate model "A" and ellipsoid artificial ignition model started in 173 degrees of rotation of the crankshaft and finished in 194 degrees. The dependence of error on each of calibrated parameters (K_1 , K_2 , and c_s) separately has somehow "parabolic-like" behaviour – it has a rather sharply separated global minimum for each set of other parameters. Obviously, the position and magnitude of the minimum change when the other parameters change. It is demonstrated on Figure 9, Figure 10, and Figure 11. The curves with "+" marks contain the best found solution (that one with least error) with the parameters:

$$K_1 = 92.0 \text{ 1/kg/s,}$$

$$c_s = 0.19,$$

$$K_2 = 292.0 \text{ 1/kg/s.}$$

The error of the best solution was 63 328 J².

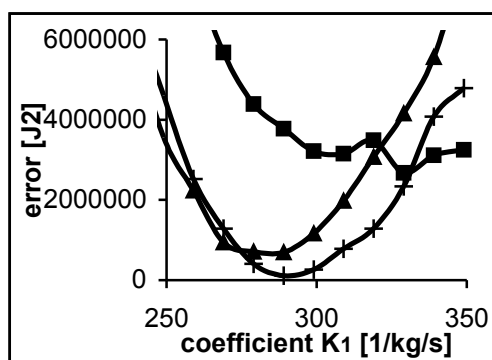


Figure 10. Selected curves of dependence of error on the coefficient K_1 . Curve with "+" marks is the one containing optimal solution.

Choice of critical temperature

Till now, the artificial ellipsoid ignition model was used to save computational time. Now, the optimal parameters will be fixed and only critical temperature T_C will be calibrated. The computations are performed with the basic reaction rate model "A" with parameters $K_1=92.0$ 1/kg/s, $c_s=0.19$, $K_2=292.0$ 1/kg/s and with natural spark ignition model with time-of-spark=start-time=173 degrees. The parameter ignition-time loses its meaning. These computations include also computation of flow field and transport of mass and energy and they are about 80 times

more time consuming than the ones with ellipsoid ignition model. 29 computations were performed.

The model is very sensitive to choice of the critical temperature. If it is set too low, the reaction starts in whole cylinder in one time, when it is set too high, the reaction does not develop out of the spark area. The limits of these two extremes are about 740 and 760 K.

Table 3. Results of calibration of start-time and ignition-time – getting time parameters (all time data are expressed in degrees of rotation of crankshaft, K_1 and K_2 are expressed in 1/kg/s)

start time [deg]	ignition time [deg]	K_1	c_s [1]	K_2	error [J ²]	error/least error
173	21	83	0.18	289	65613	1.00
173	21	90	0.20	293	65682	1.00
173	21	84	0.18	289	65846	1.00
173	21	82	0.18	289	66191	1.01
173	21	89	0.20	293	66582	1.01
173	21	85	0.18	289	66890	1.02
173	21	86	0.18	289	68384	1.04
173	21	88	0.20	293	68441	1.04
173	21	87	0.18	289	70229	1.07
173	21	87	0.20	293	71259	1.09
174	20	90	0.20	293	72448	1.10
173	21	88	0.18	289	72751	1.11
173	21	82	0.16	291	73599	1.12
173	21	82	0.18	291	73599	1.12
174	20	89	0.20	293	73905	1.13
173	21	86	0.20	293	75036	1.14
173	21	89	0.18	289	75953	1.16
174	20	88	0.20	293	76337	1.16
173	21	83	0.16	291	76813	1.17
173	21	83	0.18	291	76813	1.17
173	21	90	0.20	291	78542	1.20
173	21	85	0.20	293	79473	1.21

On Figure 12, the dependence of error on the critical temperature is drawn. There can be a cluster character of solution observed, i.e. there are intervals of parameter T_C with the same or very similar error of the solution and steep steps between such intervals, where the error rapidly

changes. The least error was obtained with parameter $T_C=749.16$ K (the error was 128234 J²). The computed curve of production of energy is drawn in Figure 13. The graphs of temperature and pressure computed by the same 0D model as \tilde{q}_a (see [5]) look in the scale of Figure 6 and Figure 7 exactly as the measured ones. The maximal difference between measured and computed pressure is 6,07%. The same maximal difference was observed in temperature data.

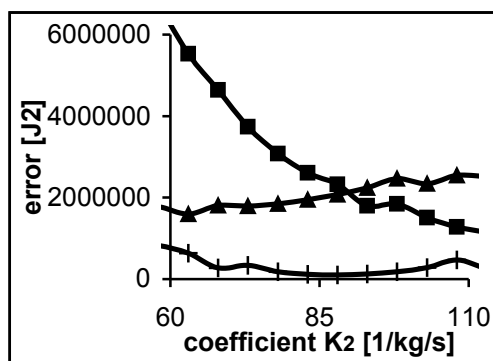


Figure 11. Selected curves of dependence of error on the coefficient K_2 . Curve with “+” marks is the one containing optimal solution.

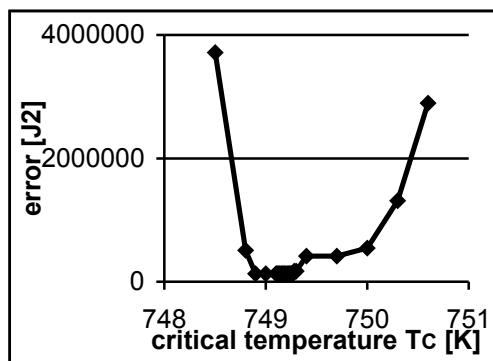


Figure 12. Dependence of error on critical temperature.

CONCLUSION

We have calibrated the simplified reaction rate model with real data. Only one parameter – the global production of energy – was optimised. The calibration showed that the parameters of the simplified local chemical model could be set so

that the numerical solution is comparable with measurement in terms of global pressure and global temperature. However, there are no local observations on progress of flame, temperature field, or flow field, there.

The problem of precise chemical models is their enormous computational time consumption. The presented simplified reaction rate model is very simple and computationally undemanding and even the critical temperature T_C is completely non-physical, we could fit it to measured data. Therefore, although many other comparisons should be done to validate the model, the presented results are hopeful.

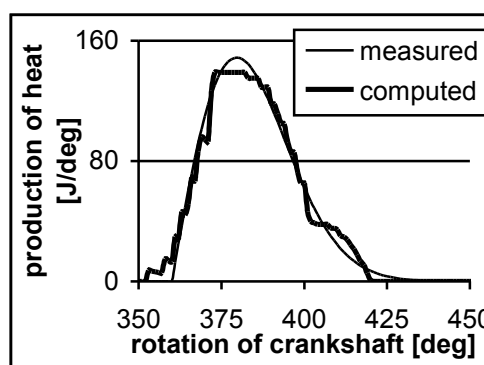


Figure 13. Result of calibration in terms of heat production.

REFERENCES

1. J. Šembera, J. Maryška, and J. Novák, FEM/FVM Modelling of Processes in Combustion Engine, In: Z. Chen, R. Glowinski, and K. Li (eds) *Current Trends in Scientific Computing*. Contemporary Mathematics, **329** (2003), pp. 291-298.
2. L. D. Landau and E. M. Lifshitz, *Fluid Mechanics*, Pergamon Press, Oxford 1982.
3. R. B. Bird, W. E. Stewart, E. N. Lightfoot, *Transport phenomena*, Wiley, New York, 2002.
4. P. Jiránek, J. Maryška, and J. Šembera, Model of Compressible Flow and Transport in a Time-Dependent Domain, Accepted to *Proceedings of Enumath 2003*, Springer Verlag, Heidelberg 2004.
5. S. Beroun, J. Blažek, T. Hájek, Z. Salhab, Computational program TLAK-macro-1101.xls – program description [in Czech], Research report SM 395/2001, TU in Liberec 2001.
http://bozek.cvut.cz/groups/publications/TLAK_TLxl.pdf